Procedia Computer Science

Volume 51, 2015, Pages 1158–1167

ICCS 2015 International Conference On Computational Science

Telescopic Projective Integration for Multiscale Kinetic Equations with a Specified Relaxation Profile

Ward Melis[1] and Giovanni Samaey[1]

Department of Computer Science, K.U. Leuven, Celestijnenlaan 200A, 3001 Leuven, Belgium
ward.melis@cs.kuleuven.be

Abstract

We study the design of a general, fully explicit numerical method for simulating kinetic equations with an extended BGK collision model allowing for multiple relaxation times. In that case, the problem is stiff and we show that its spectrum consists of multiple separated eigenvalue clusters. Projective integration methods are explicit integration schemes that first take a few small (inner) steps with a simple, explicit method, after which the solution is extrapolated forward in time over a large (outer) time step. They are very efficient schemes, provided there are only two clusters of eigenvalues. Telescopic projective integration methods generalize the idea of projective integration methods by constructing a hierarchy of projective levels. Here, we show how telescopic projective integration methods can be used to efficiently integrate multiple relaxation time BGK models. We show that the number of projective levels only depends on the number of clusters and the size of the outer level time step only depends on the slowest time scale present in the model. Both do not depend on the small-scale parameter. We analyze stability and illustrate with numerical results.

Keywords:

1 Introduction

Kinetic Boltzmann equations serve in many applications as a modeling tool on a mesoscopic level of description. In a scalar one-dimensional setting without external forcing, this equation portrays the evolution of a distribution function $f(x, v, t)$ of particles at position x with velocity v at time t, and takes the following general form:

$$\partial_t f + v\partial_x f = Q(f), \tag{1}$$

in which the left hand side corresponds to the transport of the particles whereas the collision operator Q appearing on the right hand side describes velocity changes as a consequence of interaction between particles. In general, the Boltzmann collision integral [3] is very expensive to discretize. To that end, a BGK approximation to the Boltzmann collision operator is considered instead. The collisions are modeled as a linear relaxation towards a certain Maxwellian equilibrium distribution function $\mathcal{M}_v\left(u^\epsilon\right)$ with a (small-scale) relaxation time ϵ $(0 < \epsilon \ll 1)$:

$$Q(f^\epsilon) = \frac{1}{\epsilon}\left(\mathcal{M}_v\left(u^\epsilon\right) - f^\epsilon\right). \tag{2}$$

According to this BGK approximation, particles interact with a single collision frequency given by $1/\epsilon$. A logical extension of this simple approximation is to allow for multiple distinct relaxation times. The model equation that is of interest here is a kinetic BGK equation in which we allow the relaxation time of the

 Selection and peer-review under responsibility of the Scientific Programme Committee of ICCS 2015

doi:10.1016/j.procs.2015.05.285

collisions to vary in space. This variation is embodied in a so-called relaxation profile function denoted by $\omega(x)$. We end up with the following kinetic equation:

$$\partial_t f^\epsilon + v\partial_x f^\epsilon = \frac{\omega(x)}{\epsilon}\left(\mathcal{M}_v\left(u^\epsilon\right) - f^\epsilon\right). \tag{3}$$

This relaxation profile in equation (3) can for instance be understood as the mathematical description of a composite material in which each material has its very own properties, which in a natural way leads to differing collisional relaxation times.

The difficulty of numerically integrating equations of the form (3) follows from the stiffness present on the right hand side, which restricts the choice of numerical methods. A robust and fully explicit method, which allows for time integration of (two-scale) stiff systems with arbitrary order of accuracy in time, is projective integration. Projective integration was proposed in [4] for stiff systems of ordinary differential equations with a clear gap in their eigenvalue spectrum. In such stiff problems, the fast modes, corresponding to the Jacobian eigenvalues with large negative real parts, decay quickly, whereas the slow modes correspond to eigenvalues of smaller magnitude and are the solution components of practical interest. Projective integration allows a stable yet explicit integration of such problems by first taking a few small (inner) steps (using a step size δt) with a simple, explicit method, until the transients corresponding to the fast modes have died out, and subsequently projecting (extrapolating) the solution forward in time over a large (outer) time step of size $\Delta t > \delta t$. In [9], projective integration was analyzed for kinetic equations with a diffusive scaling. An arbitrarily higher order version, based on Runge-Kutta methods, has been proposed recently in [8], where it was also analyzed for kinetic equations with an advection-diffusion limit. Alternative approaches to obtain a higher-order projective integration scheme have been proposed in [10, 11].

Projective integration methods work best whenever the problem's spectrum consists of two eigenvalue clusters (one corresponding to the fast and the other to the slow eigenvalues) with a clear spectral gap between them. When the outer time step is much larger than the inner time step, $\Delta t \gg \delta t$, the stability domain of projective integration methods consists of two circle-like stability regions [4]. In that case, the method parameters can be tuned such that (i) all fast eigenvalues of the naive time discretization of the kinetic equation fall into its first stability region and (ii) its dominant stability region contains all dominant eigenvalues. However, when we introduce a relaxation profile function $\omega(x)$ to the equations, the spectrum will in general comprise more than two eigenvalue clusters with several spectral gaps between them. The only way that stability of the method can be guaranteed then is by choosing the method parameters such that its stability region does not split up into two parts and contains both the fastest and slowest eigenvalue clusters. In that case the projective integration method is called $[0, 1]$-stable [5]. Unfortunately, this requirement completely destroys much of the potential speed-up of the method since this imposes a severe condition on the maximum possible value of the projective time step [4] thus defeating its purpose.

Clearly, projective integration methods are not suitable if the eigenvalue spectrum of the given problem contains more than two well separated eigenvalue clusters. To that end, telescopic projective integration (TPI) methods, which are presented in [5], can be used. In these methods, the outer integrator step of the classical projective integration method is seen as the inner integrator of yet another outer integrator on a coarser level. By repeating this idea, TPI methods construct a hierarchy of projective levels in which each outer integrator step on a certain level serves as an inner integrator step one level higher. The use of TPI methods remedies the aforementioned difficulty of multiple spectral gaps in two distinct ways: (i) they can be designed such that the method is always $[0, 1]$-stable with a greater speed-up than classical projective integration, or (ii) they can be set up such that there is one stability region around every eigenvalue cluster.

Here, we will construct and analyze TPI methods to integrate kinetic equations of the form (3) with a relaxation profile such that every eigenvalue cluster lies within one of the method's stability regions. The remainder of this paper is structured as follows. In section 2, we will introduce the kinetic equations, and discuss their hydrodynamic limit leading to the asymptotic equivalence with a hyperbolic problem. In section 3, we describe the telescopic projective integration method that will be used to integrate these kinetic equations. We then turn in section 4 to determining the method parameters for telescopic projective integration based on the problem's spectrum. Numerical results are reported in section 5, where we provide numerical stability results and a temporal order test of the TPI methods. We conclude in section 6.

2 Kinetic Equation and Hydrodynamic Limit

In this work, we are interested in the following (hyperbolically scaled) scalar one-dimensional kinetic equation

$$\partial_t f^\epsilon + v\partial_x f^\epsilon = \frac{\omega(x)}{\epsilon}\left(\mathcal{M}_v\left(u^\epsilon\right) - f^\epsilon\right) \tag{4}$$

modeling the evolution of a particle distribution function $f^\epsilon(x,v,t) \in \mathbb{R}$. The particle positions and velocities are denoted by $x \in \mathbb{R}$ and $v \in V \subset \mathbb{R}$ respectively, and the right hand side of (4) represents a BGK collision operator [2], modeling linear relaxation of f^ϵ to a Maxwellian distribution function $\mathcal{M}_v(u^\epsilon) \in \mathbb{R}$, in which $u^\epsilon(x,t) = \langle f^\epsilon(x,v,t)\rangle$ is the density, obtained via averaging over the measured velocity space (V,μ),

$$u := \langle f\rangle = \int_V f d\mu(v). \tag{5}$$

For the relaxation profile function $\omega(x)$ we assume $0 < \epsilon \ll \omega_{\min} \leq \omega(x) \leq \omega_{\max}$ with $\omega_{\min}$ and $\omega_{\max}$ independent of ϵ.

When assuming the following form of the Maxwellian equilibrium distribution function:

$$\mathcal{M}_v(u^\epsilon) = u^\epsilon + \frac{F(u^\epsilon)}{v}, \tag{6}$$

which complies with the following compatibility conditions on the Maxwellian:

$$\begin{cases} \langle \mathcal{M}_v\left(u\right)\rangle = u, \\ \langle v\mathcal{M}_v\left(u\right)\rangle = F(u) \end{cases}, \tag{7}$$

it is well established that the kinetic equation (4) converges in the hydrodynamic limit $\epsilon \to 0$ to the scalar one-dimensional conservation law

$$\partial_t u + \partial_x F\left(u\right) = O(\epsilon), \tag{8}$$

In what follows, we will always assume that the velocity space is discrete and of the form

$$V := \left\{v_j\right\}_{j=1}^J, \qquad d\mu(v) = \sum_{j=1}^J w_j \delta(v - v_j), \tag{9}$$

with v_j denoting the chosen velocities and w_j the corresponding weights. Due to this choice of V the kinetic equation (4) breaks up into a system of J coupled partial differential equations,

$$\partial_t f_j^\epsilon + v_j \partial_x f_j^\epsilon = \frac{\omega(x)}{\epsilon}\left(\mathcal{M}_j\left(u^\epsilon\right) - f_j^\epsilon\right), \qquad 1 \leq j \leq J, \tag{10}$$

in which $f_j^\epsilon(x,t) \equiv f^\epsilon(x,v_j,t)$, and the only coupling between different velocities is through the computation of u^ϵ. As $\epsilon \to 0$, a Chapman-Enskog expansion allows to write $f_j^\epsilon = \mathcal{M}_j\left(u^\epsilon\right) + O(\epsilon)$ so that, injecting it in (10), taking the mean value over V, and considering the relations given in (7) we obtain

$$\partial_t u^\epsilon + \partial_x F(u^\epsilon) = O(\epsilon). \tag{11}$$

3 Telescopic Projective Integration

The purpose of this paper is to construct a fully explicit, arbitrary order time integration method for the stiff system (10) containing in general more than two distinct time scales. The asymptotic-preserving property [6] implies that, in the limit when ϵ tends to zero, an ϵ-independent time step constraint, $\Delta t = O(\Delta x)$, can be used, similar to the hyperbolic CFL constraint for the limiting equation (8). To achieve this and overcome the

difficulties mentioned in the introduction, we will use an extension of the projective integration method [4,9] that can handle multiple time scales, entitled telescopic projective integration (TPI).

Telescopic projective integration employs a number of projective levels, which, starting from a base (zeroth) level integrator, are wrapped around the previous level. They form a hierarchy of projective integrators in which each level fulfills both an inner and outer integrator role (except of course for the first and last level). This clearly generalizes the idea of projective integration, which contains only one projective level wrapped around an inner integrator. On that account, in the TPI framework the projective integration method is called a level-1 TPI method. The idea of a level-2 TPI scheme is sketched in figure 1.

The different level integrators can in principle be selected independently from each other, but in general one selects a first order explicit scheme (e.g., the forward Euler scheme) for all but the outermost integrator level, which is selected to meet certain accuracy requirements dictated by the problem.

3.1 TPI Method Parameters

In general, the level-m TPI method possesses a (possibly varying) set of parameters corresponding to all of its levels. This includes: (i) the level-i integrator time step $h_i,\ i = 0, ..., m$, (ii) the number of level-i integrator iterations $K_i,\ i = 0, ..., m-1$ that are needed to sufficiently damp the fast components on each level, (iii) the extra number of level-i integrator iterations $q_i,\ i = 0, ..., m-1$ used to approximate the derivative and perform the extrapolation, and (iv) the number of level-i integrator steps $M_i,\ i = 0, ..., m-1$ over which the level-$(i+1)$ integrator is applied and thus skipped by all of the underlying level integrators.

Note that the level-0 (innermost) integrator time step h_0 is the only 'real' time step of the method meaning that this is the only step over which numerical integration is actually performed. All higher level time steps are merely the consequence of the K-, q- and M-values of the extrapolation. Once h_0 is known, the projective time steps are calculated by the following relation:

$$h_{i+1} = \prod_{k=0}^{i} (M_k + K_k + q_k) h_0, \qquad i = 0, ..., m-1 \tag{12}$$

Additionally, we notice that for $m = 1$ the (level-1) TPI method coincides with the classical PI method.

3.2 Innermost Integrator

We intend to integrate the system of equations (10) on a uniform, constant in time, periodic spatial mesh with spacing Δx, consisting of I mesh points $x_i = i\Delta x$, $1 \le i \le I$, with $I\Delta x = 1$, and a uniform time mesh with time step h_0, i.e., $t^k = kh_0$. After discretizing in space, we obtain the following semi-discrete system of ordinary differential equations:

$$\dot{\mathbf{f}} = \mathrm{D}_t(\mathbf{f}), \qquad \mathrm{D}_t(\mathbf{f}) := -\mathrm{D}_{\mathbf{x},\mathbf{v}}(\mathbf{f}) + \frac{\boldsymbol{\omega}}{\epsilon} \left(\mathcal{M}_v(\mathbf{u}) - \mathbf{f} \right), \tag{13}$$

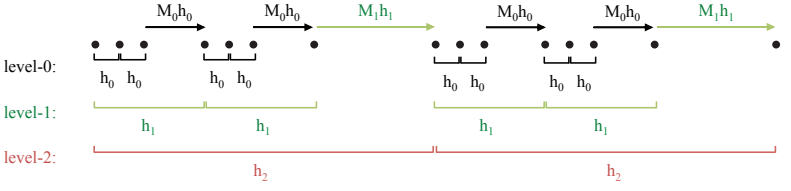

Figure 1: Sketch of the general idea of a level-2 telescopic projective integration method drawn for two complete outer steps h_2 of the method. The dots correspond to the different time points at which the numerical solution is calculated. The time step and projective step size of each level are denoted by h_i and M_i respectively.

in which $\mathbf{f}$ and $\boldsymbol{\omega}$ are vectors of length $I \times J$ and where $\mathrm{D}_{x,v}(\cdot)$ represents a suitable discretization of the first order spatial derivative $v\partial_x$ (e.g., upwind differences). The innermost (so-called level-0) integrator of the TPI method is chosen to be an explicit scheme, for which we use the following shorthand notation

$$\mathbf{f}^{k+1} = S_0(\mathbf{f}^k), \qquad k = 0, 1, \ldots \tag{14}$$

in which S_0 denotes the time stepper of the level-0 integrator with step size h_0. The forward Euler (FE) method immediately comes to mind:

$$\mathbf{f}^{k+1} = \mathbf{f}^k + h_0 \mathrm{D}_t(\mathbf{f}^k). \tag{15}$$

3.3 Projective (Outer) Levels

The telescopic projective integration method employs a number m of nested projective levels that are constructed outwards with the innermost integrator as its fundamental building block. We will here provide the scheme of the method in a framework similar to that of classical projective integration.

To keep track of the time instant at which the numerical solution is computed throughout the TPI method and at the same time desiring a compact notation, in what follows we employ superscript triplets of the form (i, n, k) in which i denotes the integrator level, n corresponds to the index of the outermost time instants $t^n = nh_m$ and k represents the iteration index of the current level-i integrator. In addition to this, we introduce a local time such that the time to which the superscript triplets point is with respect to this local time and not with respect to the beginning of the current level-m integration step.

Starting from a computed numerical solution $\mathbf{f}^n$ at time $t^n = nh_m$, one first takes $K+1$ steps of size h_0 with the level-0 integrator,

$$\mathbf{f}^{0,n,k+1} = S_0(\mathbf{f}^{0,n,k}), \qquad 0 \le k \le K, \tag{16}$$

in which $\mathbf{f}^{0,n,k}$ corresponds to the numerical solution at time $t^{0,n,k} = t^{1,n}_{\mathrm{loc}} + kh_0$ calculated by the level-i integrator. In the projective integration framework the scheme is set up from the highest level down to the lowest level. The aim is to obtain a discrete derivative to be used in the *level-m projective* step to compute $\mathbf{f}^{n+1} = \mathbf{f}^{m,n+1,0}$ via extrapolation in time. This leads to:

$$\mathbf{f}^{m,n+1,0} = \mathbf{f}^{m-1,n,K+1} + (h_m - (K+1)h_{m-1}) \frac{\mathbf{f}^{m-1,n,K+1} - \mathbf{f}^{m-1,n,K}}{h_{m-1}}, \qquad t^{m,n}_{\mathrm{loc}} = nh_m. \tag{17}$$

From equation (17) we observe that this scheme requires the solution calculated by the (lower) level-$(m-1)$ integrator. For $i = 1, ..., m-1$ the lower level-i integrator schemes can be written in a similar way as follows:

$$\mathbf{f}^{i,n,k} = \mathbf{f}^{i-1,n,K+1} + (h_i - (K+1)h_{i-1}) \frac{\mathbf{f}^{i-1,n,K+1} - \mathbf{f}^{i-1,n,K}}{h_{i-1}}, \quad t^{i,n}_{\mathrm{loc}} = t^{i+1,n}_{\mathrm{loc}} + kh_i, \quad k = 0, ..., K. \tag{18}$$

This method is called telescopic projective forward Euler (TPFE), and it is the simplest instantiation of this class of integration methods.

3.4 Stability of Telescopic Projective Integration

We now briefly discuss the main stability properties of the TPFE method. To this end, we introduce the test equation and its corresponding innermost integrator,

$$\dot{y} = \lambda y, \qquad y^{k+1} = \tau(\lambda \delta t) y^k, \qquad \lambda \in \mathbb{C}. \tag{19}$$

As in [4], we call $\tau(\lambda\delta t)$ the *amplification factor* of the innermost integrator. (For instance, if the inner integrator is the forward Euler scheme, we have $\tau(\lambda\delta t) = 1 + \lambda\delta t$.) The inner integrator is stable if $|\tau| \le 1$. The question then is for which subset of these values the TPI method is also stable. Considering the level-m TPFE method, it can easily be seen from equations (17)-(18) that it is stable if

$$|\sigma_m(\tau)| = \left| \left((M_{m-1}+1)\sigma_{m-1}(\tau) - M_{m-1} \right) \left(\sigma_{m-1}(\tau) \right)^{K_{m-1}} \right| \le 1, \tag{20}$$

in which σ_i denotes the level-i integrator amplification factor. Equation (20) needs to hold for all eigenvalues τ of the innermost integrator.

Here, we consider the level-m TPI method with constant $q_i = 1$ and variable M_i and K_i, $i = 0, ..., m-1$. Since we are interested in the limit $\epsilon \to 0$ for fixed Δx, we look at the limiting stability regions (i.e. $M_i \to \infty$). In this regime, the following result holds [5]:

Theorem 3.1. *The level-m TPI method contains $m+1$ (principal) regions of stability around the real axis, which can be positioned to cover the clusters of eigenvalues by choice of (possibly) different K_i-, q_i- and M_i-values at each projective level. Furthermore, there are a number of artifact stability regions due to the value of K, which can not be tuned independently and are of no importance whatsoever.*

The TPI method allows for the accurate integration of solution modes within the dominant stability region while maintaining stability for all other modes by matching its stability regions around the reasonably well separated eigenvalue clusters of the problem's spectrum.

4 Numerical Properties

4.1 Spectrum of the Innermost Integrator

We now turn to the specific goal of determining the spectrum of the innermost integrator of the TPI method for which we will consider a simple forward Euler scheme. To do so we will first calculate the spectrum of the semi-discretized kinetic equation (13) under study. From these eigenvalues the spectrum of the innermost integrator can be derived.

First, consider the case of a constant function $\omega(x) = \bar{\omega} \in \mathbb{R}$. We start by rewriting the semi-discretized kinetic equation (13) in the (spatial) Fourier domain,

$$\partial_t \hat{\mathbf{F}}(\zeta) = \boldsymbol{\mathcal{B}}\, \hat{\mathbf{F}}(\zeta) \qquad \boldsymbol{\mathcal{B}} = \frac{\bar{\omega}}{\epsilon}\left(\mathbf{MP} - \mathbf{I} + \frac{\epsilon}{\bar{\omega}}\mathbf{D}\right), \tag{21}$$

in which $\hat{\mathbf{F}} \in \mathbb{R}^J$, the matrices $\boldsymbol{\mathcal{B}}$, $\mathbf{M}$, $\mathbf{P} \in \mathbb{R}^{J\times J}$, and $\mathbf{I}$ represents the identity matrix of dimension J. In (21), the matrix $\mathbf{D}$ represents the (diagonal) Fourier matrix of the spatial discretization, which depends on the Fourier mode ζ, $\mathbf{P}$ is the Fourier matrix of the averaging of f over all velocities, and the matrix $\mathbf{M} = \mathbf{I} + \mathbf{V}^{-1}$ represents the Fourier transform of the Maxwellian, with $\mathbf{V}$ the diagonal matrix with elements v_j.

To locate the spectrum, we will need to assume that the velocity space is symmetric, i.e.,

$$v_{J-j+1} = -v_j \text{ and } D_{J-j+1} = \bar{D}_j, \qquad 1 \le j \le J/2. \tag{22}$$

Moreover, we write, from now on, $D_j = \alpha_j + \imath\beta_j$. The following theorem is a corollary to [8, Theorem 4.1].

Theorem 4.1. *Under the above assumptions, the spectrum of the matrix $\boldsymbol{\mathcal{B}} = \frac{\bar{\omega}}{\epsilon}\left(\mathbf{MP} - \mathbf{I} + \frac{\epsilon}{\bar{\omega}}\mathbf{D}\right)$ satisfies*

$$\mathrm{Sp}(\boldsymbol{\mathcal{B}}) \subset \mathcal{D}\left(-\frac{\bar{\omega}}{\epsilon}, C\right) \cup \{\lambda(\epsilon, \bar{\omega})\} \tag{23}$$

where the constant C depends on the parameters $\boldsymbol{\alpha} = (\alpha_j)_{j=1}^J$ and $\boldsymbol{\beta} = (\beta_j)_{j=1}^J$ of the spatial discretization scheme and the chosen velocities $\mathbf{v} = (v_j)_{j=1}^J$. The dominant eigenvalue $\lambda(\epsilon, \bar{\omega})$ is simple and can be expanded as

$$\Re(\lambda(\epsilon, \bar{\omega})) = \langle \boldsymbol{\alpha} \rangle + \frac{1}{\bar{\omega}}\left(\langle \boldsymbol{\alpha}^2 \rangle - \langle \boldsymbol{\alpha} \rangle^2 - \langle \boldsymbol{\beta}^2 \rangle + \left\langle \frac{\boldsymbol{\beta}}{\mathbf{v}} \right\rangle^2\right)\epsilon, \tag{24}$$

$$\Im(\lambda(\epsilon, \bar{\omega})) = \left\langle \frac{\boldsymbol{\beta}}{\mathbf{v}} \right\rangle. \tag{25}$$

When $\omega(x)$ is a piecewise constant function over the spatial domain consisting of m constant values or 'levels' $\bar{\omega}_i$, $i = 1, ..., m$, the above expressions in the Fourier domain rapidly become very difficult for in this case the equations contain convolutions. However, we are still able to get an idea of the spectrum of the (formal) amplification matrix $\tilde{\boldsymbol{\mathcal{B}}}$ by performing numerical experiments. These experiments suggest that the spectrum of $\tilde{\boldsymbol{\mathcal{B}}}$ consists of (i) a combination of the m fast spectra obtained when considering constant $\omega(x) = \bar{\omega}_i$ for all x and this for every $i = 1, ..., m$, and (ii) the dominant eigenvalues $\lambda(\epsilon, \bar{\omega}_1)$ given by (24)-(25), in which $\bar{\omega}_1$ is considered to be the largest ω-level. Therefore, using result (23), we formally write the following result on the spectrum of $\tilde{\boldsymbol{\mathcal{B}}}$:

$$\mathrm{Sp}(\tilde{\boldsymbol{\mathcal{B}}}) \subset \left\{ \bigcup_{i=1}^{m} \mathcal{D}\left(-\frac{\bar{\omega}_i}{\epsilon}, C_i\right) \cup \{\lambda(\epsilon, \bar{\omega}_1)\} \right\}, \tag{26}$$

in which each of the constants C_i depends on $\boldsymbol{\alpha}$, $\boldsymbol{\beta}$ and $\mathbf{v}$. An illustration of the spectrum is shown on the left hand side of figure 2. Details of this experiment can be found in section 5.1.

When we write the Fourier transform of the innermost forward Euler scheme (15) as

$$\hat{\mathbf{F}}^{k+1} = \mathbf{S}_0\, \hat{\mathbf{F}}^k = \left(\mathbf{I} + h_0 \tilde{\boldsymbol{\mathcal{B}}}\right) \hat{\mathbf{F}}^k, \tag{27}$$

it is clear that the amplification factors $\boldsymbol{\tau} = (\tau_1, \ldots, \tau_J)$ of the forward Euler scheme, which are the eigenvalues of $\mathbf{S}_0$, and the eigenvalues $\boldsymbol{\lambda} = (\lambda_1, \ldots, \lambda_J)$ of the matrix $\tilde{\boldsymbol{\mathcal{B}}}$ are related via

$$\tau_j = 1 + h_0 \lambda_j, \qquad 1 \leq j \leq J. \tag{28}$$

(By convention, we consider the dominant eigenvalue $\lambda(\epsilon, \bar{\omega}_1) = \lambda_1$.) Thus, the spectrum of an inner forward Euler time-stepper satisfies

$$\mathrm{Sp}(\mathbf{I} + h_0 \tilde{\boldsymbol{\mathcal{B}}}) \subset \left\{ \bigcup_{i=1}^{m} \mathcal{D}\left(1 - \frac{h_0 \bar{\omega}_i}{\epsilon}, O(\epsilon)\right) \cup \{1 + h_0 \lambda(\epsilon, \bar{\omega}_1)\} \right\}, \tag{29}$$

with $\lambda(\epsilon, \bar{\omega})$ given in theorem 4.1.

4.2 TPI Method Parameters

This section is concerned with the selection of the TPI method parameters K_i and M_i such that the TPI method is stable. The starting point is a given eigenvalue spectrum containing $m+1$ eigenvalue clusters with m fast and 1 slow eigenvalue cluster, which are all located in the left half plane of the complex λ-plane. The aim of this section is to construct a concrete strategy for determining the time steps K_i and M_i-values of the TPI method from the (semi-discretized) problem's spectrum such that we end up with a stable method.

The underlying idea is the following. For $i = 0, ..., m-1$ the purpose of the level-i integrator is to bring the i^{th} fast eigenvalue cluster to 0 (i.e. the level-i integrator should damp all eigenvalues in the i^{th} fast cluster) whereby the i faster-than-the-current eigenvalue clusters, which were already around 0 due to the application of the lower level integrators still remain around 0 and are suppressed even more by the level-i integrator. We can design the values M_i such that the the current (i^{th}) eigenvalue cluster is maximally damped. The $m - i$ remaining eigenvalue clusters to the right of the current cluster will shift somewhat more to the left (i.e. towards 0) since the level-i integrator is also (slightly) damping these eigenvalues. For stability reasons we require that the remaining $m-i$ clusters still lie in the stability region of the level-$(i+1)$ integrator. This can be achieved by carefully selecting the values K_i.

It is clear that in the above reasoning we only desire a stable numerical integration of the fast modes. The dominant modes, which are the solution components of interest, on the other hand need to be integrated both in a stable and accurate way. Underneath we scrutinize the level-m TPI method construction. The analysis will be carried out assuming the forward Euler method on levels $i = 0, ..., m-1$. The outermost (level-m) integrator can be any stable explicit method depending on the required accuracy.

Level-0 integrator. The innermost integrator of the TPI method is the forward Euler scheme with time step h_0. As explained in the introduction of this section we will fix h_0 such that the fastest eigenvalue cluster with center λ_0 is moved to 0 in the complex τ-plane. Using equation (28), this leads to $h_0 = 1/|\lambda_0|$. This choice of the time step h_0 defines a linear mapping of eigenvalues λ to (level-0) eigenvalues τ, which can be found in the complex τ-plane within the interval $[-\eta, 1]$ with $\eta \in \mathbb{R}^+$ close to zero.

Level-i integrator. For $i = 1, ..., m-1$ the level-i integrator is the projective forward Euler (PFE) scheme [4], which extrapolates the solution of its inner integrator (i.e. the level-$(i-1)$ integrator) over a distance $M_{i-1}h_{i-1}$. Its amplification factor σ_i in terms of its inner integrator amplification factor σ_{i-1} is given by:

$$\sigma_i(\sigma_{i-1}) = \big((M_{i-1}+1)\sigma_{i-1} - M_{i-1}\big)\sigma_{i-1}^{K_{i-1}} \tag{30}$$

with $\sigma_0 \equiv \tau$. After applying the level-$(i-1)$ integrator there will be $m+2-i$ eigenvalue clusters in the σ_{i-1}-plane of which there are $m+1-i$ fast and 1 slow cluster, and i clusters will already have been brought around 0 by the lower level integrators turning these into one big cluster around 0. We then demand that M_{i-1} is chosen such that the fastest eigenvalue cluster that is not yet around 0 in the σ_{i-1}-plane will be moved to 0 in the σ_i-plane. This cluster is denoted by $\sigma_{i-1,i}$, in which the notation $\sigma_{k,l} = \sigma_k(\lambda_l)$ represents the transformation of eigenvalue cluster λ_k to the σ_l-plane. Using expression (30) we find:

$$M_{i-1} \mid \sigma_i(\sigma_{i-1,i}) = 0 \Rightarrow M_{i-1} = \frac{\sigma_{i-1,i}}{1-\sigma_{i-1,i}}. \tag{31}$$

Once M_{i-1} is known, we fix the value of K_{i-1} by demanding that all fast eigenvalue clusters that are already around 0 in the σ_{i-1}-plane fall into the projective level-i stability region around 0 which is given by $\mathcal{D}(0, (1/M_{i-1})^{1/K_{i-1}})$ [4] where $\mathcal{D}(\kappa, \mu)$ denotes the disk with center $(\kappa, 0)$ and radius μ. We thus obtain:

$$\sqrt[K_{i-1}]{1/M_{i-1}} \geq \hat{\sigma}_{i-1} \Rightarrow K_{i-1} = \left\lceil \frac{\log(1/M_{i-1})}{\log(\hat{\sigma}_{i-1})} \right\rceil, \tag{32}$$

in which $\hat{\sigma}_{i-1} = \max_{k\in\{0,1,...,i-1\}} |\sigma_{i-1,k}|$. It is clear that both M_{i-1} and K_{i-1} are independent of ϵ.

Level-m integrator. Finally, the level-m or outermost integrator is designed by ensuring that the real part of the fastest eigenvalue of the dominant eigenvalue cluster denoted by $\tilde{\sigma}_{m-1,m}$ in the σ_{m-1}-plane falls in the dominant stability region of the level-m integrator, which is given by the region $\mathcal{D}(1-1/M_{m-1}, 1/M_{m-1})$ [4]. This leads to the following inequality:

$$\Re(\tilde{\sigma}_{m-1,m}) \geq 1 - \frac{2}{M_{m-1}}. \tag{33}$$

To obtain M_{m-1} we examine how the expression of the fastest dominant eigenvalue in the σ_0-plane, which will remain the fastest dominant eigenvalue in all other σ_i-planes, is transformed by the projective integrators. This eigenvalue in the complex σ_0-plane is given in equation (29). In case of upwind differences of order 1 in space it is of the following form: $\tilde{\sigma}_{0,m} = 1 - \tilde{C}_0 h_0$ where $\tilde{C}_0 = 2\langle|v|\rangle/\Delta x$. By plugging the expression of $\tilde{\sigma}_{0,m}$ into equation (30) we find that for $i = 1, ..., m-1$ the i^{th} level PFE integrator scheme transforms this eigenvalue into:

$$\tilde{\sigma}_{i,m} \approx 1 - \tilde{C}_i h_0, \qquad \tilde{C}_i = \tilde{C}_0 \prod_{k=0}^{i-1} (M_k + K_k + 1). \tag{34}$$

Using equation (34) we can now use the condition given in (33) to find the value of M_{m-1}. To this end, we will turn the inequality in (33) into an equality. The corresponding (maximal allowed) value of M_{m-1} is

$$M_{m-1} = \frac{2}{\tilde{C}_{m-1} h_0}. \tag{35}$$

Once the value of M_{m-1} is known we use equation (32) to determine the corresponding value of K_{m-1}.

5 Numerical Experiments

5.1 Stability Results

We begin by demonstrating the idea of obtaining a stable TPI method as outlined in section 4.2. To that end, we consider the kinetic equation (3) with a piecewise constant relaxation profile containing 4 different well separated ω-values $\{1, 0.01, 0.001, 0.0001\}$ and $\epsilon = 10^{-6}$. We consider the Maxwellian $\mathcal{M}_v(u) = u + u/v$ corresponding to the flux function $F(u) = u$ of the linear advection equation. The velocity space is discretized using $J = 2$ velocities $\{v_1, v_2\} = \{1.01, -1.01\}$.

The spectrum will be calculated for $x \in [0, L]$, using $L = 1$ together with periodic boundary conditions. Since there are 4 ω-levels, we will construct a stable level-4 TPI method. The innermost integrator is a space-time discretization of equation (3), in which we choose the standard upwind scheme of order 1 with grid spacing $\Delta x = 10^{-2}$, combined with a forward Euler time discretization with $h_0 = \epsilon$.

Using equations (31), (35) and (32) we obtain the following values for $M_i,\ i = 0, ..., 3$: 9, 8.17, 8.03 and 4.12 and K_i: 1, 1, 1 and 2. The stability regions (green) together with the eigenvalues (blue crosses) in each plane are shown on the left hand side of figure 2. In each complex σ_i-plane, $i = 0, ..., 3$ we also plotted the (asymptotic) stability regions (red dashed circles) of the level-$(i+1)$ projective integration method. We observe that all level-i eigenvalues fall in these asymptotic regions. Moreover, notice that in the σ_4-plane the stability region coincides with the unit disc and all σ_4-eigenvalues lie within this region.

5.2 Order Test

We now illustrate the order of the TPI method in time. To this end, we consider the Maxwellian $\mathcal{M}_v(u) = u + u/v$ leading to the linear advection equation on the macroscopic scale.

We compute the solution for $t \in [0, 0.02]$ and $x \in [0, L]$, using $L = 1$. We impose periodic boundary conditions and choose a smooth initial condition: $u(x, 0) = \exp\left(-160(x - 1/2)^2\right)$. We compute the error E at time $t = 0.02$ by taking the 1-norm of the difference between the numerical solution and the analytical solution of the (linear) semi-discretized system (13). By doing so we take into account the discretization error in space such that we only look at the error in time.

For the relaxation method, we use the kinetic equation (3) with 3 different well separated ω-levels, in which we discretize the velocity space using $J = 2$ velocities $(v_1, v_2) = (1.01, -1.01)$. The TPI method consists of 3 projective levels since there are three ω-values. The innermost integrator is a space-time discretization of equation (3), in which we choose the standard upwind scheme of order 3 with grid spacing $\Delta x = 10^{-2}$, combined with a forward Euler time discretization with $h_0 = \epsilon$ and $\epsilon = 10^{-8}$. The values of M_i and $K_i,\ i = 0, ..., 2$ on each level are determined such that the method is stable.

For demonstrating the temporal order of the TPI method we will vary the outermost time step h_3. The simulations are run for PFE, PRK2 and PRK4 as outermost integrators. All other projective level integrators correspond to the PFE method. The result can be seen on the right hand side of figure 2. On this plot, we observe that the error curves level off for small values of h_3 in the case of PRK2 and PRK4 as outermost integrators. This is due to the fact that the contribution of the temporal discretization error becomes negligible, and the error due to the approximation of the time derivative in each projective step by a finite difference approximation becomes dominant. The numerical error of the latter approximation cannot be decreased further than $O\left(\sqrt{\epsilon_{mach}}\right)$ with $\epsilon_{mach} \approx 10^{-16}$ being the machine precision. This is precisely what we observe on the left hand side plot.

6 Conclusions

We presented a general, fully explicit integration method for kinetic equations with BGK source term containing multiple relaxation times. Unlike other methods based on relaxation [1, 7], the telescopic projective integration method does not rely on a splitting technique, but only on an appropriate selection of time steps using a naive explicit discretization method at its core. Its main advantage is its generality and ease of use.

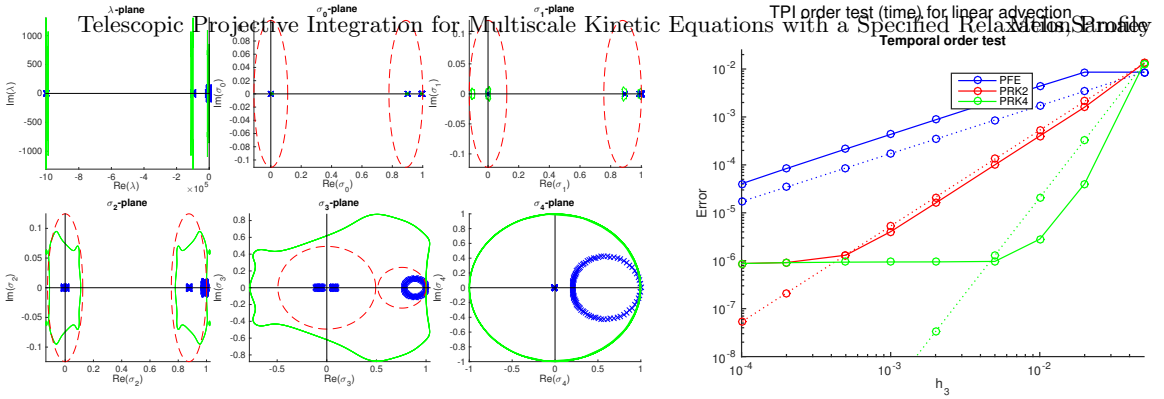

Figure 2: Left: stability analysis for a level-4 TPI method. Blue crosses in each plane correspond to eigenvalues in that plane. Green regions represent the stability regions of the full level-4 TPI method with respect to the plane under study. The red dashed regions are the stability regions of the projective integration method of the next level integrator in a certain plane. Right: order test in time for a level-3 TPI method. Solid lines: numerical error curves calculated with the 1-norm. Dotted lines: expected error curve for a particular order.

We showed that, with an appropriate choice of inner step size, the time step restriction on the outer time step is independent of the small-scale parameter. Moreover, the number of projective levels is also independent of the scaling parameter. We analyzed stability, and illustrated with numerical results.

For future work, we foresee to elaborate on the application of a time-dependent relaxation profile function. In that case, the problem's spectrum changes with time and as a result the TPI method parameters will also be time-dependent. Alternatively, one could construct a TPI method using a fixed set of parameters containing only one stability region encompassing all eigenvalues. This of course yields a less efficient method.

References

[1] D. Aregba-Driollet and R. Natalini. Discrete kinetic schemes for multidimensional systems of conservation laws. *SIAM Journal on Numerical Analysis*, 37(6):1973–2004, 2000.

[2] P.L. Bhatnagar, E.P. Gross, and M. Krook. A model for collision processes in gases. I. Small amplitude processes in charged and neutral one-component systems. *Physical review*, 94(3):511, 1954.

[3] C. Cercignani. *The Boltzmann Equation and Its Applications*, volume 1979. Springer New York, 1988.

[4] C.W. Gear and I.G. Kevrekidis. Projective methods for stiff differential equations: problems with gaps in their eigenvalue spectrum. *SIAM Journal on Scientific Computing*, 24(4):1091–1106, 2003.

[5] C.W. Gear and I.G. Kevrekidis. Telescopic projective methods for parabolic differential equations. *Journal of Computational Physics*, 187(1):95–109, 2003.

[6] S. Jin. Efficient asymptotic-preserving (AP) schemes for some multiscale kinetic equations. *SIAM Journal on Scientific Computing*, 21(2):441–454, 1999.

[7] S. Jin and Z. Xin. The relaxation schemes for systems of conservation laws in arbitrary space dimensions. *Communications on pure and applied mathematics*, 48(3):235–276, 1995.

[8] P. Lafitte, A. Lejon, and G. Samaey. A high-order asymptotic-preserving scheme for kinetic equations using projective integration. *Submitted*, 2014.

[9] P. Lafitte and G. Samaey. Asymptotic-preserving projective integration schemes for kinetic equations in the diffusion limit. *SIAM Journal on Scientific Computing*, 34(2):579–602, 2012.

[10] S.L. Lee and C.W. Gear. Second-order accurate projective integrators for multiscale problems. *J. Comput. Appl. Math.*, 201(1):258–274, 2007.

[11] R. Rico-Martınez, C.W. Gear, and I.G. Kevrekidis. Coarse projective kMC integration: forward/reverse initial and boundary value problems. *J. Comput. Phys.*, 196(2):474–489, 2004.